Lohan *et al.*
Future Journal of Pharmaceutical Sciences (2023) 9:117
https://doi.org/10.1186/s43094-023-00572-3

Future Journal of Pharmaceutical Sciences

RESEARCH Open Access

Optimization and evaluation of microwave-assisted curcumin-loaded nanostructured lipid carriers: a green approach

Sunidhi Lohan[1], Ravinder Verma[2], Deepak Kaushik[3] and Meenakshi Bhatia[1*]

Abstract

Background The goal of current research work is to develop and optimize curcumin-encapsulated nanostructured lipid carriers and to enhance therapeutic effect of curcumin after oral administration.

Method Curcumin-loaded nanostructured lipid carriers were developed by a single-step one-pot microwave-assisted technique. The preparation of curcumin-loaded nanostructured lipid carriers was optimized by employing two factors and three levels central composite design (Design Expert® software) taking concentration of lipid blend and surfactant as independent variables and particle size, polydispersity index, and zeta potential as dependent variables, to investigate the effect of formulation ingredients on the physicochemical characteristics of nanostructured lipid carriers. The optimized batch was investigated by Fourier transform infrared spectroscopy, differential scanning calorimetry, X-ray diffraction, high-resolution transmission electron microscopy, in vitro drug release, stability studies, cytotoxicity, and in vivo anthelmintic studies.

Results The average particle size, polydispersity index, and zeta potential of the optimized batch were found to be 144 nm, 0.301, and − 33.2 mV, respectively, with an entrapment efficiency of 92.48%. The results of high-resolution transmission electron microscopy confirmed spherical shape of particles. In vivo antiparasitic studies included determining the duration of paralysis and eventual death of earthworms in the presence of test samples. The results of in vivo studies showed good anthelmintic potential for curcumin-loaded nanostructured lipid carriers as compared to albendazole in different concentrations. Cytotoxicity studies also confirmed the formulation to be nontoxic to Vero cells. In vitro drug release study showed 90.76 ± 0.01% release of curcumin in 24 h by following the Korsmeyer-Peppas model of release kinetics.

Conclusion The aforementioned results imply that microwave-developed nanostructured lipid carriers could be promising drug carriers and will aid in their fabrication for oral administration as a possible alternative for the treatment of other parasitic infections.

Highlights

- Curcumin-loaded nanostructured lipid carriers (Cr-NLCs) were prepared by a fast and easy single-step one-pot microwave-assisted technique.
- Implementation of 2 factors at 3 levels with central composite design (Design Expert® software) to investigate the influence of the formulation ingredients on the physicochemical properties of the NLCs.

*Correspondence:
Meenakshi Bhatia
meenaxibhatia@gmail.com
Full list of author information is available at the end of the article

- Optimized batch of Cr-NLC demonstrated nanosized particles with improved drug release characteristics, excellent entrapment efficiency and augmented physical stability.
- The anthelmintic potential of Cr-NLC was determined by a study on earthworms and was compared with albendazole.
- A cytotoxicity study was performed on Vero cells and evaluated in terms of IC_{50} value.

Keywords Antiparasitic, Curcumin, Cytotoxicity, Microwave-assisted production, Nanostructured lipid carriers, Vero cells

Graphical Abstract

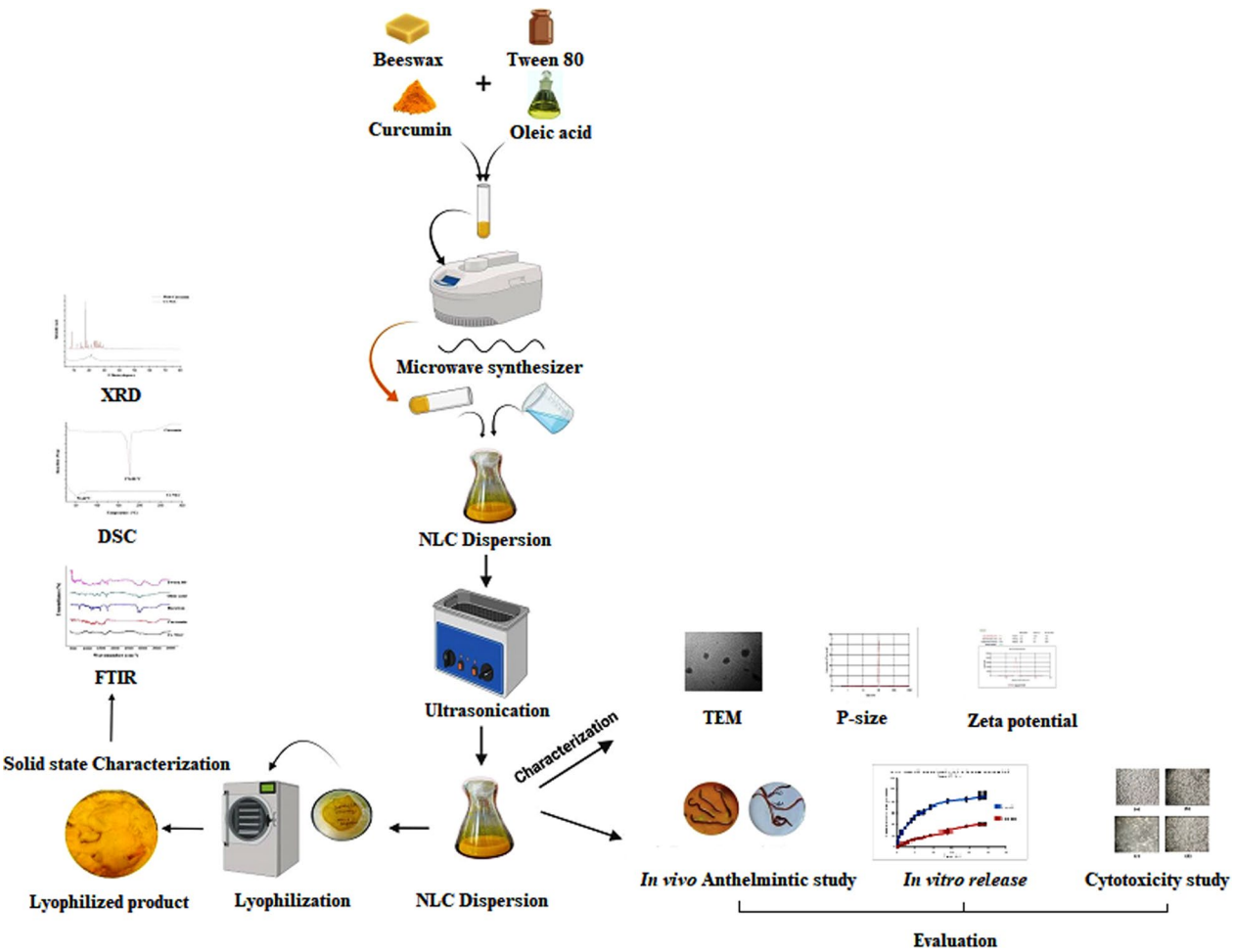

Background

Parasitic infections remain to be a cause of major concern in various parts of the world, mostly in developing countries due to inadequate control measures. Soil-transmitted helminth infections are among the most common human parasitic infections globally mainly caused by tapeworms and roundworms affecting the underprivileged and poor populations having limited access to potable water, sanitation, and hygiene [1, 2]. To combat parasitic infections, medicinal plants are one of the most effective treatment approaches since ancient times [3, 4]. Natural bioactive, curcumin

obtained from the rhizome of the plant *Curcuma longa L*, (*C. longa*) belonging to the family *Zingiberaceae* is well known for its anti-inflammatory, antimicrobial, anticancer, antioxidant, antiparasitic, neuroprotective, and other properties [5, 6]. Curcumin has antibacterial properties that are effective against viruses, parasites, bacteria, and fungi and anthelminthic activity against helminth infections has been reported [7, 8]. Curcumin is a water-insoluble, yellow-colored, polyphenolic, crystalline powder with high lipophilicity and is commonly known as a golden nutraceutical [9, 10]. Due to poor aqueous solubility, fast metabolism, and instability in some physiological conditions, oral administration of curcumin shows limited and declined therapeutic benefits [11]. To improve its therapeutic efficiency and eliminate biological barriers nanotechnology is well appreciated in the biomedical and pharmaceutical fields [12, 13]. With unique biological, chemical, structural, mechanical, magnetic, and electrical properties, nanoparticles offer various benefits in treating human ailments [14, 15]. As biological, chemotherapeutic, and immunotherapeutic agents' nanomedicines play a vital role in the treatment of several ailments [16, 17]. Over the past few decades lipidic colloidal carriers, like liposomes, emulsions, solid lipid nanoparticles (SLNs), and nanostructured lipid carriers (NLCs), etc. have been studied extensively [18, 19]. However great attention has been focused on NLCs owing to reduced particle size, easy preparation techniques, nontoxicity, stability, biocompatibility, the possibility of scale-up, less-ordered crystalline structure, amended drug loading, and less surfactant is required for the production of stable NLCs, etc. [20, 21]. Lipids are the main constituents of NLCs that affect drug loading capability, stability and sustained release behavior of the pharmaceutical preparation. Compared to other lipid materials such as fatty acids, triglycerides, or partial glycerides, wax-based NLCs have received less research attention [22, 23]. Waxes are simple esters of fatty acids that contain long-chain alcohols. It has been reported that wax-based lipid nanoparticles show excellent particle size distribution and more physical stability. Beeswax is an important biocompatible natural wax that mainly contains palmitate, hydroxypalmitate, palmitoleate, and oleate esters of long-chain (C_{30}–C_{32}) aliphatic alcohols [24]. Several techniques have been established for the formulation of nanostructured lipid carriers including double emulsion/solvent evaporation [25], high-pressure homogenization [26], emulsification followed by homogenization [27], simple hot-emulsion and ultrasonication [28], phase inversion, solvent emulsification-evaporation, and solvent injection [29], etc. In recent times, a novel microwave-assisted one-pot single-step, easy, and fast technique has been reported to formulate nanoparticles. It is an effective, clean, simple, and speedy process that allows "uniform heat penetration and gradient temperature as compared to conventional techniques of localized heating, thus fabricating nanoparticles of more uniform size and low polydispersity index" (PdI) [30]. In the present study, single step, one-pot microwave-assisted method of preparation entrapping curcumin was used to fabricate different batches of NLC employing 2 factors 3 levels of central composite design (CCD) having solid & liquid lipid blend (beeswax and oleic acid) and concentration of surfactant as independent variables with p-size, PdI, and zeta potential as dependent ones. After preparation, the optimized batch was characterized by FTIR, XRD, DSC, and TEM studies, and further cytotoxicity studies, in vitro and in vivo evaluation was carried out. The objective of current research work was to formulate and optimize curcumin-encapsulated NLCs to improve its therapeutic potential as an antiparasitic agent, by utilizing fast and eco-friendly techniques including microwave synthesis [31].

Methods

Materials

Beeswax, cholesterol, stearic acid, and oleic acid were acquired from Sisco Research Laboratories Private Limited Mumbai, India. Curcumin and Tween 80 were procured from Loba Chemie Pvt. Ltd. Mumbai, India. Earthworms (*Pheretima posthuma*) were obtained from *the Department* of *Agronomy*, *CCSHA*U Hisar, India. Other analytical-grade chemicals and reagents were used as they were received.

Screening of solid and liquid lipids

The solubility of the drug in solid lipid, liquid lipid, and surfactant is required to achieve adequate drug loading in the NLC system [32, 33]. Therefore, studies on lipid solubility laid down the solubility of curcumin in lipids. Briefly, 2 mg of curcumin was added in solid lipid (beeswax/cholesterol/stearic acid, separately) and heated up to 80 °C. Increasing amounts of solid lipids were added until the insoluble curcumin disappeared in the melted lipids. The amount of solid lipid required to completely solubilize the drug was determined [34]. Based on solubility studies beeswax was selected as solid lipid. However selection of liquid lipid and surfactant was based on previous reports. Here, oleic acid was selected as liquid lipid being biodegradable, economical, and nontoxic [35–37]. However, Tween 80 was selected as a favorable nonionic surfactant (having high solubilization capacity, low toxicity, and low cost) [38, 39].

Preparation of curcumin-loaded NLC

Curcumin-NLCs (Cr-NLC) were prepared by a novel microwave-assisted single-pot technique [40, 41]. Preliminary trials were conducted to determine the upper and lower concentration of beeswax and oleic acid (in the ratio of 1:9 to 9:1) that formed desired NLCs. Briefly, beeswax, oleic acid, and curcumin (10% of lipid blend) were heated with Tween 80 (2–4% *w*/*v*) at 80 °C under constant stirring (600 rpm) for 10 min at a power not exceeding 18W in a Monowave 200, microwave reactor (Anton Paar GmbH, Austria) [42–44]. The resulting nanoemulsion was dispersed into water by sonicating for 30 min using a Power Sonic 405, ultrasonic bath sonicator (Hawashin, Seoul, Korea) to prepare curcumin NLC dispersion (Fig. 1).

Experimental design

The Cr-NLC formulation was optimized using a two-factor, three-level CCD [45]. The concentration of lipid blend (X_1) (2–6%) and concentration of surfactant (X_2) (2–4%) were selected and taken into consideration at three different levels (−1, 0, 1). The average p-size (Y_1), PdI (Y_2), and zeta potential (ζ) (Y_3) were designated as responses (Table 1). The experimental data were analyzed statistically using Design-Expert® software version 13 (Stat-Ease Inc. Minneapolis, Minnesota) [46]. Scaling up was done for the selected batch keeping the drug/lipid/surfactant ratio constant and average p-size, PdI, and zeta potential were determined.

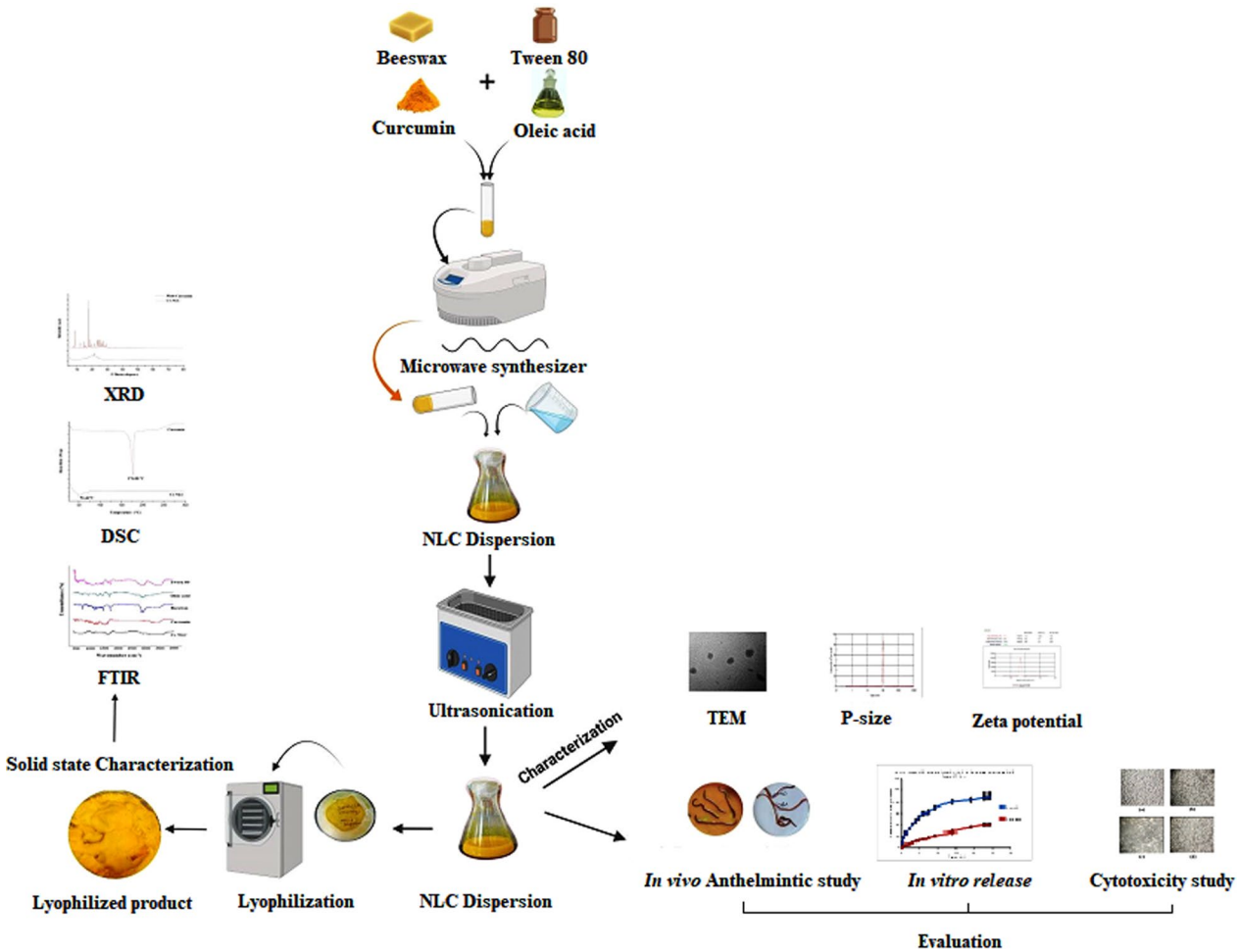

Fig. 1 Schematic representation of formulation, characterization and evaluation of Cr-NLC

Table 1 Variables and levels for CCD

Factor	Levels		
Independent variables	1	0	−1
Concentration of lipid blend (% w/w) (X_1)	6	4	2
Concentration of surfactant (% w/v) (X_2)	4	3	2
Dependent variables	*Constraints*		
P-size (nm)(Y_1)	Minimize		
PdI (Y_2)	Minimum		
Zeta potential (mV) (Y_3)	In range		

Characterization of curcumin NLC

P-size, PdI, and zeta potential

The determination of average p-size, PdI, and zeta potential (ζ) of all batches of Cr-NLC was carried out by a dynamic light scattering method via a Zetasizer Nano ZS90, (Particle size analyzer from Malvern Instruments, UK). The sample was measured in triplicate using an automatic mode at a 90° angle while allowing 120 s for equilibration [47].

Encapsulation efficiency (%EE)

% EE of all the batches was calculated by the method already reported [34, 48]. Large particles and unentrapped curcumin were separated from the Cr-NLC dispersion by centrifuging it at 6000 rpm for 6 min. Supernatant was subjected to an additional 15 min of 15,000 rpm centrifugation for the separation of curcumin nanoparticles from the dispersion. The supernatant was decanted, and the drug content was determined at λmax of 425 nm using the UV–visible spectrophotometer. The following equation (Eq. 1) was used to calculate the %EE:

$$\text{Entrapment efficiency}(\%) = \frac{(\text{Total Drug Content} - \text{Drug Content in Supernatant})}{\text{Total Drug Content}} \times 100 \quad (1)$$

Transmission electron microscopy

The morphological characteristics of the selected Cr-NLC formulation were investigated by TEM. A drop of the Cr-NLC dispersion was applied to a copper grid that had been coated with carbon and allowed to dry at room temperature after being diluted 1:10(*v*/*v*) with deionized water [47]. Then, the sample was observed by Zeiss EM 900, transmission electron microscope.

In vitro drug release investigation

The optimized formulation of Cr-NLC dispersion was used to study in vitro drug release of curcumin, using a dialysis membrane (12–14 kDa) in USP-II type dissolution apparatus (Electrolab Dissolution Tester, 2,109,048, India) at 37 ± 0.5 °C. The Cr-NLC dispersion was incorporated to pre-activated dialysis membrane and immersed in 300 ml of phosphate buffer (pH 6.8) as release media and stirred at 100 rpm. The aliquots (5 mL) were collected at predetermined time points for 24 h and replenished with an equal volume of fresh release media [49]. All the collected aliquots were analyzed with UV–Visible spectrophotometer at λ_{max} 425 nm. The experiment was performed in triplicate [38, 50]. Similarly, the release of curcumin from aqueous dispersion was also determined. The release data were fitted in to different release kinetic models (zero order, first order, Higuchi and Korsmeyer-Peppas) to detect the mechanism of drug release.

Solid state characterization

The optimized batch of Cr-NLC dispersion was lyophilized (Alpha-2–4 LD Plus model, Martin Christ, Germany) for solid-state characterization by differential scanning calorimetry (DSC), X-ray diffraction (XRD) and Fourier transforms infrared (FT-IR) spectroscopy.

Differential scanning calorimetry (DSC)

Thermal analysis of pure curcumin and lyophilized samples of the optimized batch of Cr-NLC was carried out by Shimadzu DSC-60 Plus, differential scanning calorimeter (TA-60WS thermal analyzer) over the range of 30–300 °C at a heating rate of 10 °C/min. The nitrogen gas was constantly used to purge the sample at a flow rate of 30 ml/min throughout measurement, to maintain the inert environment of the experiment [51].

Fourier transform infrared spectroscopy

The FT-IR spectrum of beeswax, oleic acid, Tween 80, pure curcumin, and lyophilized Cr-NLC formulation were recorded to perceive any interactions between drug and formulation excipients. The IR spectra were scanned in the 400–4000 cm^{-1} range using the KBr pellet method at a resolution of 1 cm^{-1} [51].

X-ray diffraction

The X-ray diffractograms of the samples were recorded by D8 Advance diffractometer by employing primary monochromatic radiation (Cu Kα1, $\lambda = 1.5406$ Å) generated at 40 kV(voltage), and 40 mA(current) with a step

size of 0.05°/s and a range of 5°–40° 2θ [52]. The crystallinity index of NLC was calculated using the Scherrer equation as given below (Eq. 2):

$$\text{Degree of crystallinity} = \frac{\text{Area of crystalline peaks}}{\text{Area of all peaks}} \times 100 \quad (2)$$

Stability study of Cr-NLC

A Stability study is a key step to assess the capacity of the formulated product to maintain its chemical and physical properties on storage. The stability studies carried out as per the recommendation of ICH guidelines are very advantageous in maintaining the safety, quality, and efficiency of formulated products throughout the shelf life. The formulated Cr-NLCs dispersion was evaluated for stability studies for 90 days at 4 °C and 25 °C. After 90 days, preparations were assessed for p-size, PdI, % entrapment efficiency and zeta potential (ζ) in triplicate [53].

Anthelmintic assay

The anthelmintic assay was performed on earthworms due to its close anatomical and physiological similitude with human intestinal parasites [54, 55]. The anthelmintic activity was carried out as described by Ajayieoba et al. with slight modifications [56]. Briefly, 15 ml aqueous dispersions of pure curcumin, Cr-NLC, and albendazole at two different concentrations (10 and 20 mg/ml) were taken in different Petri dishes. Each Petri dish was placed with Indian earthworms (*Pheretima posthuma*, weighing approximately, 4 g each) and observed for paralysis or death, for a maximum period of 60 min. Saline was used to maintain negative control. All experiments were carried out thrice. The paralysis time (min) was recorded when the worms showed no movement except when disturbed with the help of a glass rod and the death time (min) was noted as the time when no movement of worms was observed after shaking or even immersing in water.

Cytotoxicity assay

The cytotoxicity study (in vitro) of Cr-NLC was performed and compared with the pure curcumin "using the 3-(4, 5-dimethylthiazol-2-yl)-2, 5-diphenyl tetrazolium bromide (MTT) test" as per established technique [57]. *MTT assay* is a simple, sensitive and fast technique for cytotoxicity testing. Briefly, Vero cells were cultured on 96-well plates, and after 24 h in a humid incubator at 70% confluence, the cells were subjected to escalating quantities of curcumin and Cr-NLC in the concentration range of 10, 20, 40, 60 and 80 µg/ml. The media in each well was removed after 24 h and MTT (5 mg/ml) was added before being incubated for 3 h at 37 °C. A Bio-Rad microplate reader was used to measure the optical density of the formazan solution at a wavelength of 570 nm. The values of IC_{50} (Half-maximal inhibitory concentration, i.e., drug concentration inhibiting 50% of cell growth.), demonstrating cytotoxicity of each formulation, were computed [57]. Every set of experiments was carried out in triplicate.

Results

NLCs entrapping curcumin were successfully prepared by a microwave-assisted, one-step, single-pot technique using Central Composite Experimental Design (Design Expert® software). Nanoemulsion contains beeswax and oleic acid as solid and liquid lipids, Tween 80 (HLB 16) as surfactant, and the concentration of drug curcumin (0.4%) is kept constant in each formulation. All the ingredients used for the fabrication of NLCs are GRAS listed [58].

Experimental design

Particle size, PdI, zeta potential, and % EE

Beeswax and oleic acid were used as solid and liquid lipids, respectively, in the ratio of 7:3. Here, in this study 2 factors, 3-level CCD was employed containing a concentration of lipid blend (2–6%, X_1) and concentration of surfactant (2–4%, X_2) as independent variables whereas PdI, p-size, and zeta potential (ζ) were chosen to be dependent variables (Table 2). The p-size, PdI, and zeta potential (ζ) of each batch of NLC formulation were determined and are displayed in Table 2. The % EE of all the batches lies in the range from 92.4 ± 0.2%

Table 2 Formulation constraints and responses for CCD

Batch No	Concentration of lipid blend (% *w/w*) (X_1)	Surfactant (% *w/v*) (X_2)	P-size (nm) (Y_1)	PdI (Y_2)	Zeta Potential (ζ) (mV) (Y_3)
1	6	4	346.3	0.416	−31.6
2	4	3	249	0.371	−31.2
3	4	3	244.3	0.341	−29.8
4	4	3	236	0.363	−29.6
5	4	3	225	0.354	−31.4
6	2	3	266	0.408	−28.8
7	2	2	346.8	0.467	−25.3
8	4	3	256	0.38	−29.2
9	4	4	144	0.301	−33.2
10	4	2	311	0.432	−26.8
11	6	3	460	0.47	−27.8
12	6	2	520	0.508	−26.9
13	2	4	244	0.361	−32.3
Scale up	20	20	130	0.279	−33

to 98.3 ± 0.3%, thus depicting that each batch possesses a handsome amount of drug entrapped. The p-size range varies from 144 to 520 nm with monodispersity of the formulation (PdI value between 0.301 and 0.508), also the value of zeta potential of all the batches lies in the range of − 25.3 to − 33.2 mV. However, batch 9 containing 4% lipid blend and 4% surfactant has come out to be an optimized batch based on the value of p-size(144 nm), PdI (0.301), and zeta potential (− 33.2 mV) that is suggested by the Design by taking constraints applied (i.e., p-size and PdI to be minimum) into consideration.

The Cr-NLCs were optimized using central composite design. The purpose of the experimental design was to investigate the influence of variations in the surfactant and lipid blend on the physicochemical properties of Cr-NLCs such as p-size, PdI, and zeta potential. Additionally, utilizing the experimental design protocol (Design Expert 13), response data were fitted into various polynomial models. The particle size varied from 144 to 520 nm for the experimental runs. The particle size was affected by the variation in concentration of lipid blend and surfactant. The 3D plot indicates (Fig. 2) that the dependent and independent variables have a curvilinear relationship. Moreover, the plot demonstrates that a higher concentration of Tween 80 and mid value of lipid blend favors the lower particle size. It was found that a quadratic model without any data alteration provided the best match for the response P-size (Y_1). Equation 3 can also be used to express the polynomial model for the responses average p-size (Y_1), with determination correlations (R^2) of 0.9833. The synergistic and antagonistic effects are described by positive (+) and negative (−) coefficient values for particular variables in the following polynomial equation.

$$Y_1 = 239.88 + 78.25X_1 - 73.92X_2 - 17.72X_1X_2 + 128.58\,X_1^2 - 6.9\,X_2^2 \quad (3)$$

Adequate precision of average p-size was found to be 31.81 showing an adequate signal. Since the measurement of the signal-to-noise ratio, or sufficient precision, is far higher than required value of 4, model fit aids the model in navigating the design space.

The PdI ranged from 0.301 to 0.508. The 3D plot indicates that the dependent and independent variables have a curvilinear relationship. Moreover, the plot (Fig. 3) demonstrates that a higher concentration of Tween 80 and mid value of lipid blend favors the less PdI. It was found that a quadratic model without any data alteration provided the best match for the response PdI (Y_2). The polynomial equation obtained for the PdI (Y_2) is provided in Eq. 4 with the determination correlation of predicted R^2 of 0.8657 in closer agreement with the adjusted R^2 of 0.9451 (difference < 0.2). Adequate precision of PdI was found to be 22.0179 indicating an adequate signal. Equation 4 can also be used to express the polynomial model for the response PdI (Y_2) with determination correlations (R^2) 0.9680.

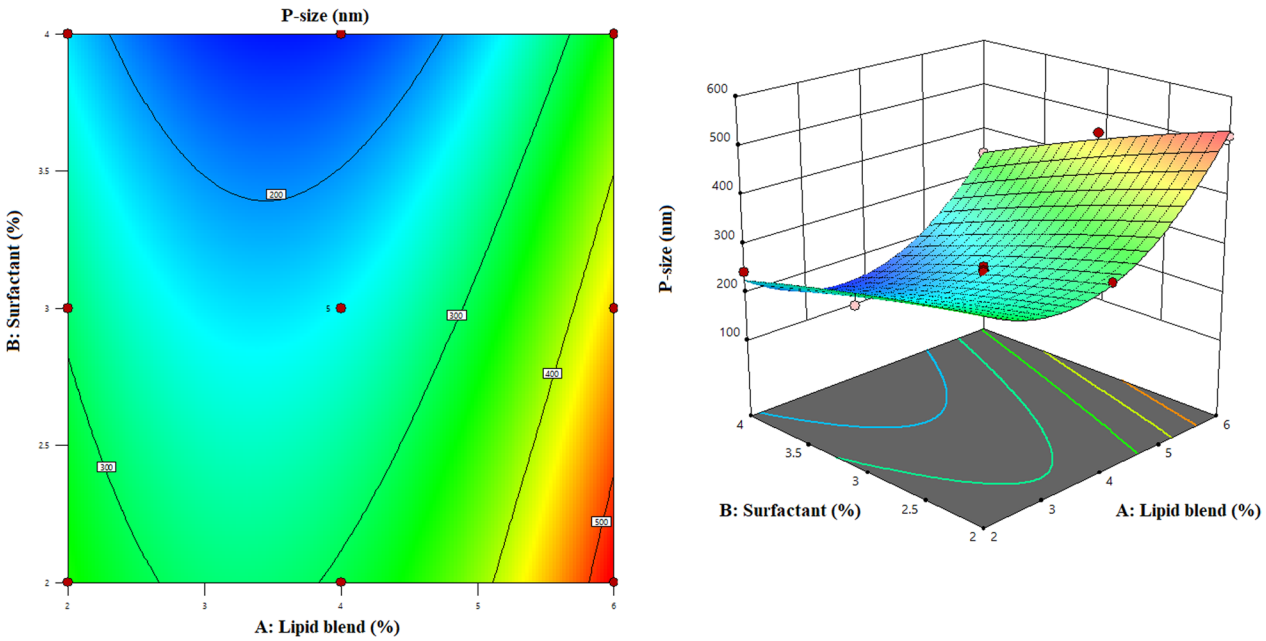

Fig. 2 Contour and 3D plot showing combined effect of lipid blend and surfactant on the particle size

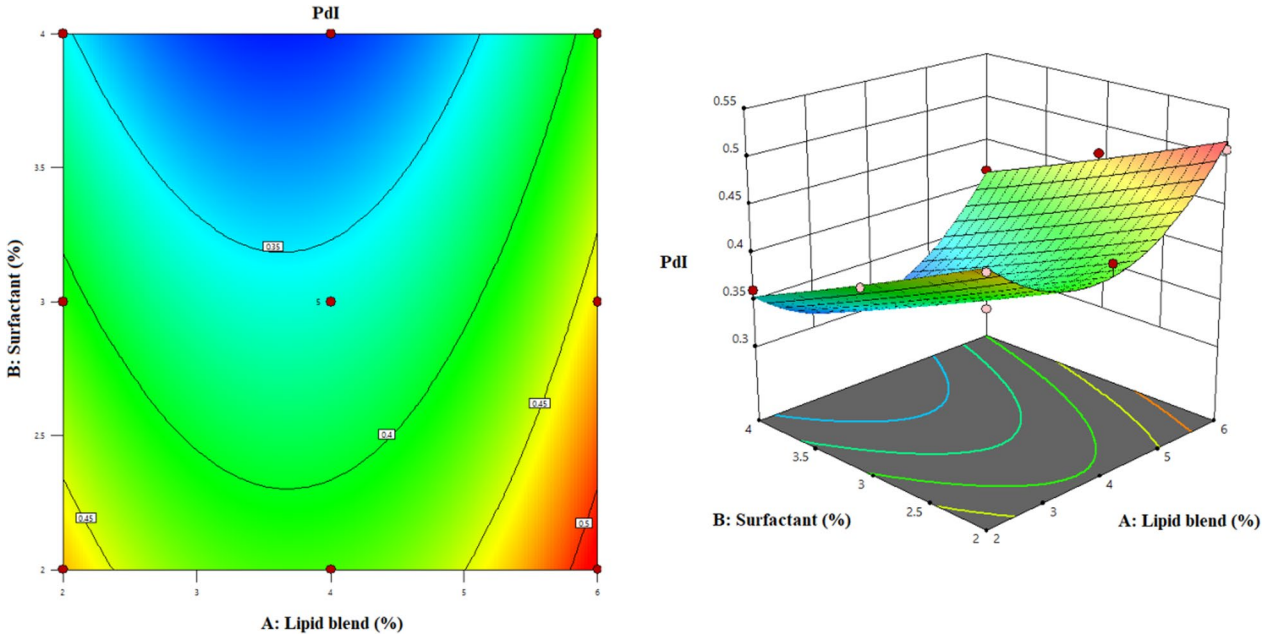

Fig. 3 Contour and 3D plot showing combined effect of lipid blend and surfactant on the PdI

$$Y_2 = 0.3626 + 0.0263X_1 - 0.0548X_2 + 0.0035X_1X_2 + 0.0744\,X_1^2 + 0.0019\,X_2^2 \quad (4)$$

It was found that a quadratic model without any data alteration provided the best match for the response zeta potential (Y_3). Equation 5 can also be used to express the polynomial models for the response zeta potential (Y_3), with determination correlations (R^2) 0.9203. Adequate precision of zeta potential was found to be 13.52 indicating an adequate signal. The polynomial equation obtained for zeta potential is presented in Eq. 5. The anticipated R^2 has a strong correlation with the adjusted

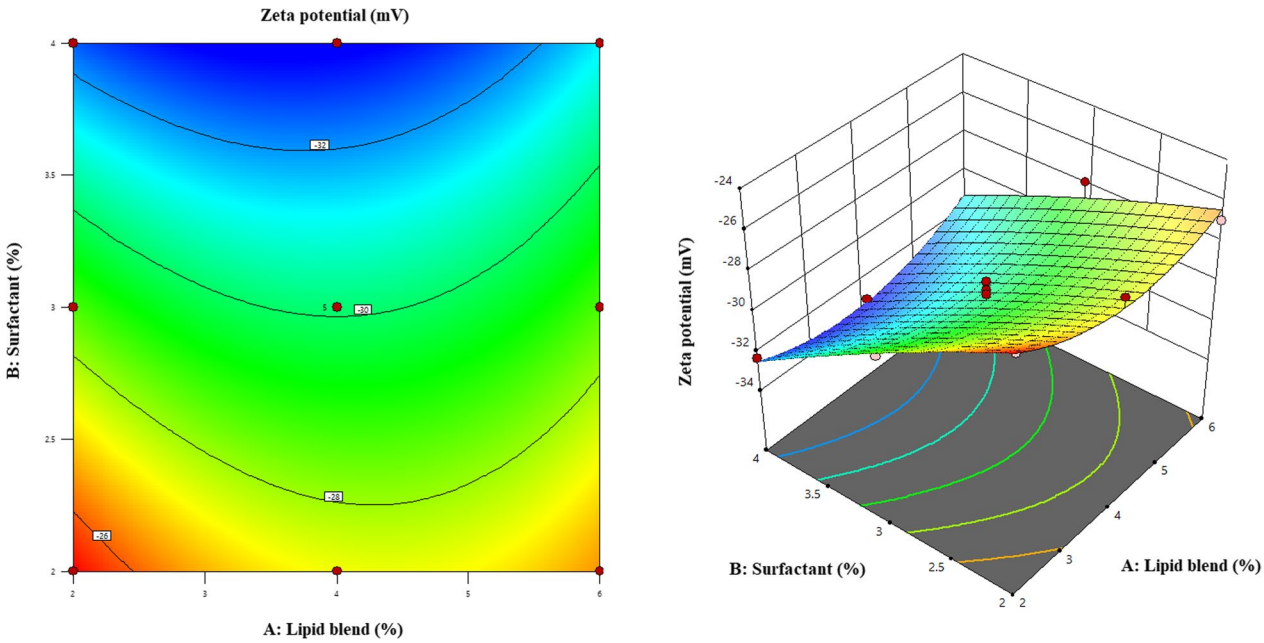

Fig. 4 Contour and 3D plot showing combined effect of lipid blend and surfactant on the zeta potential

Table 3 Statistics for the model

Responses	Model					Lack of fit	
	F-value	Prob. > f	R^2	Adeq.Prec	C.V. (%)	F-value	Prob. > f
P-size	82.29	0.0001	0.9833	31.8113	5.82	3.48	0.1296
PdI	42.34	0.0001	0.9680	22.0179	3.48	0.6281	0.6340
Zeta potential	16.16	0.0010	0.9203	13.5226	2.97	0.4871	0.7095

R^2 (difference < 0.2). The synergistic and antagonistic effects are described by positive (+) and negative (–) coefficient values for particular variables in the following polynomial equations (Fig. 4).

$$Y_3 = -30.11 + 0.0167X_1 - 3.02X_2 + 0.5750X_1X_2 + 1.47X_1^2 - 0.2259X_2^2 \quad (5)$$

Table 3 provides a summary of the results of ANOVA on selected responses. The response surface model (RSM) demonstrated that the model was significant ($P < 0.0500$). The observed and anticipated responses are well correlated, as shown by the R^2 (> 0.9) value.

Optimization

Based on a quadratic model, the optimization Eqs. 3, 4, and 5 entailing the dependent and independent elements were amassed. To the dependent variables or responses, the desirability function was used with constraints to achieve a lower level of P-size, PdI, and a higher level of zeta potential, batch 9 came out to be an optimized batch. To fabricate the NLC mathematical optimization tool with the desirability approach was used. The concentration of lipid blend (3.541%) and concentration of surfactant (3.942%) were the parameters suggested by the design that provides NLC with a P-size of 152.7 nm (predicted value 156.742), PdI 0.275 (predicted value 0.310) and zeta potential − 33.2 mV (− 33.2 mV predicted value). The RSM built from the suggested final concentration of the surfactant and lipid blend did not show any considerable differences ($P < 0.05$) between the observed and anticipated values for any of the responses based on the data. The strong predictive capability of the model was demonstrated by the closer agreement between expected and observed values.

High-resolution transmission electron microscopy (HR-TEM)

The optimized batch of Cr-NLC was exposed to transmission electron microscopy, and the images obtained are exhibited in Fig. 5. The HR-TEM images displayed spherical particles in the size range of 10–200 nm.

Studies on in vitro drug release

In vitro drug release profile of curcumin from Cr-NLCs and curcumin aqueous dispersion is shown in Fig. 6. The cumulative amount of drug release revealed a biphasic release pattern of the curcumin from the optimized batch of Cr-NLC. In the first 1 h, there was an initial burst release of about 24.48 ± 0.01% curcumin was perceived which was followed by a sustained release (90.76 ± 0.01%) in 24 h. The burst effect may be a result of the release of therapeutic agent that was adsorbed on surface of the NLC, and prolonged release effect may be caused by drug molecules diffusing into dissolution media through the lipid matrix of the NLC [59]. On the other hand, the curcumin solution demonstrated only 40.22 ± 0.01% release of the drug in 24 h. The release data was fitted into

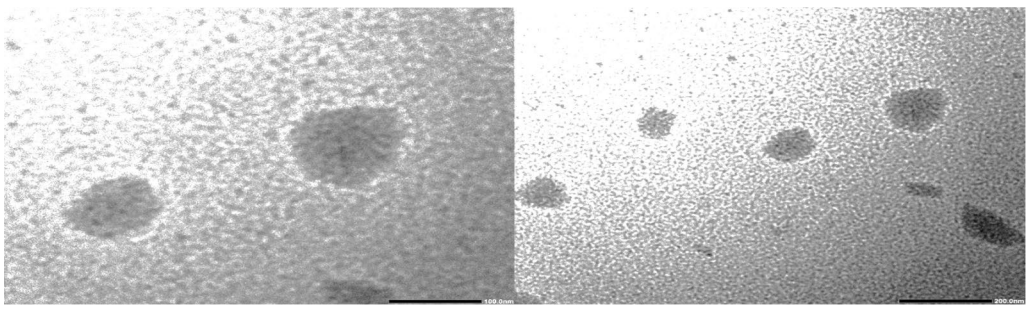

Fig. 5 HR-TEM of Cr-NLC

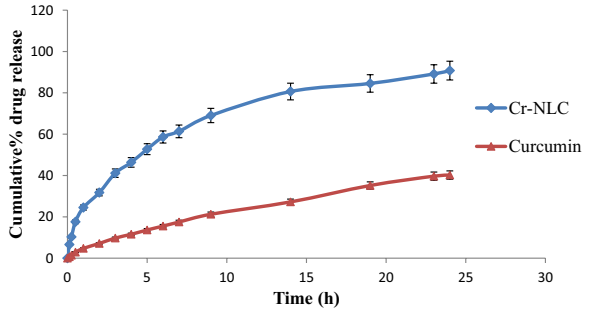

Fig. 6 In vitro release of curcumin from Cr-NLC and curcumin dispersion at pH 6.8 at 37 ± 0.5 °C

different release kinetic models and value of R^2 comes out to be 0.825, 0.434, 0.974 and 0.984 for zero order, first order, Higuchi and Korsmeyer-Peppas models, respectively. However, the optimized batch of Cr-NLC dispersion followed the Korsmeyer-Peppas model of release kinetics (R^2 0.984) following Fickian diffusion as the mechanism of the drug release from the formulation (with $n = 0.4 < 0.5$).

Interpretation of solid state characterization

Fourier transform infrared spectroscopy (FTIR)

Figure 7 displays the FTIR spectra of Tween 80, oleic acid, beeswax, curcumin, and Cr-NLC. The peaks in the FT-IR spectra of pure curcumin were found at 3511 cm^{-1} (-OH stretch), 2975 cm^{-1} (–CH_3 Asymmetric stretch) 1628 cm^{-1} (overlapping stretching vibrations of alkenes (–C=C), and carbonyl (–C=O) group), 1510 cm^{-1}(enol –OH), 1457 cm^{-1} (–CH_2, asymmetric stretching), 1429 cm^{-1} (–C=C aromatic stretching vibration), 1281 cm^{-1} (Phenol-OH) and 1115 cm^{-1} (–CO Stretching). In FTIR spectra of oleic acid, distinctive peaks were seen at 3007 cm^{-1} (–CH stretch in –C=C–H), 2926 cm^{-1} (–CH_2 asymmetric stretching), 2854 cm^{-1} (–CH_2 symmetric stretching), 1711 cm^{-1} (–C=O stretch),1464 cm^{-1} (in-plane –OH band), 1413 cm^{-1} (–CH_3 umbrella mode), 1285 cm^{-1} (–CO stretch), 937 cm^{-1} (out of the plane –OH stretch). The FTIR spectra of Tween 80, showed characteristic peaks at 3465 cm^{-1} (strong band hydroxyl stretching vibrations), 2919 cm^{-1} (asymmetric stretching band of –CH_2), 1732 cm^{-1} (stretching band due to –C=O ester group), 1249 cm^{-1} (–CO stretching vibrations). FTIR spectra of beeswax displayed three vibrations in the 2849–2956 cm^{-1} region, which is caused by the –C–H stretching of the methyl (–CH_2) and methylene (–CH_3) groups. "The band at 1732 cm^{-1} is attributed to the –C=O stretching vibration of the carboxylic groups involved in an ester linkage" [77]. Other peaks of beeswax FTIR are found at 1464 cm^{-1} (–CH_2 scissor deformation), 1175 cm^{-1} (–C=O stretching and –C–H bending vibrations), and 719 cm^{-1} (–CH_2 rocking mode). In the FTIR spectra of Cr-NLC formulation broadening of peaks was observed. It was confirmed that the peak of 3511.38 cm^{-1} became wider and flatter, indicating that the hydrogen bond was enhanced [60]. Further, FTIR spectra revealed that there is no chemical interaction between drug and the formulation excipients.

Differential scanning calorimetry (DSC)

The DSC thermogram of pure curcumin exhibited an endothermic peak at 176.88 °C pertaining to its melting point (Fig. 8). On the other hand, the DSC thermogram of Cr-NLCs revealed that endothermic peak of curcumin vanished because of transformation from crystalline to

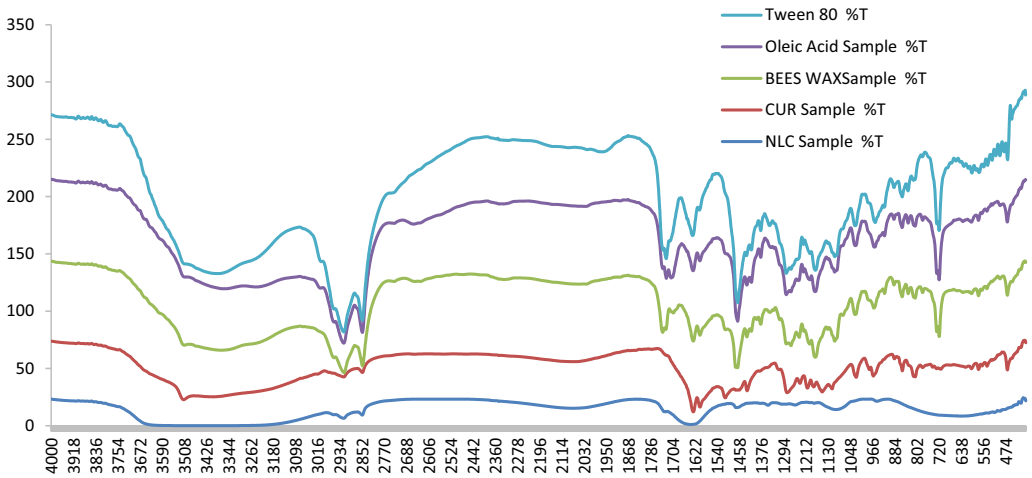

Fig. 7 FTIR spectra of Tween 80, oleic acid, beeswax, curcumin, and Cr-NLC

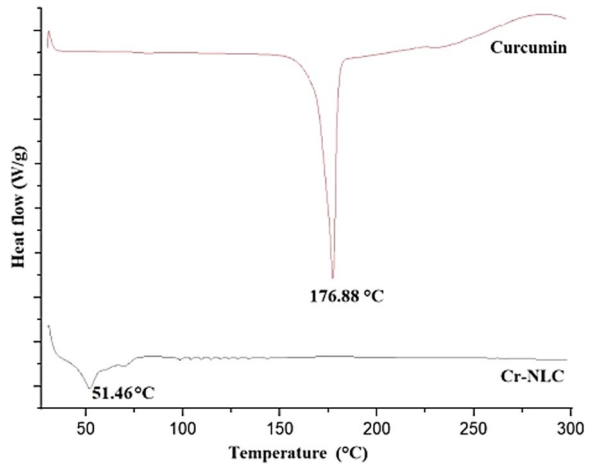

Fig. 8 DSC thermogram of curcumin and Cr-NLC

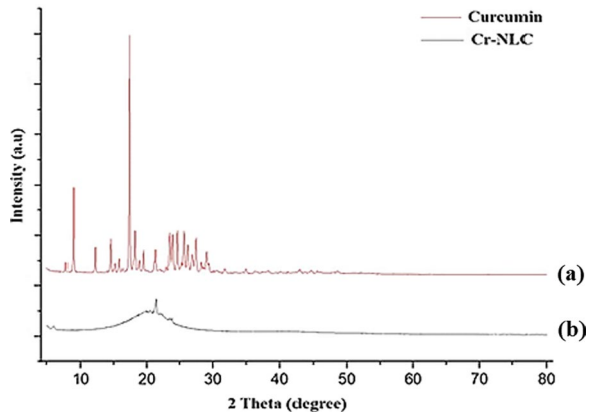

Fig. 9 XRD spectra of **a** curcumin and **b** Cr-NLC

amorphous form "which was anticipated due to the solubility of curcumin in solid and liquid lipid matrix during the fabrication of NLC in microwave" [61].

X-ray diffraction

The X-ray diffractogram of Cr-NLC and plain curcumin is shown in Fig. 9. The XRD pattern of pure curcumin showed well-defined, intense sharp peaks of 8.79731°, 12.69608°, 14.92704°, 17.158°, 24.95554°, 26.08185°, 27.74966°, and 29.13589° at 2Θ indicating the crystalline nature of the material, whereas XRD spectra of Cr-NLC displayed a more disordered or amorphous state of the formulation. The amorphous form has enhanced water solubility due to higher Gibbs free energy [62]. The crystallinity index (Ic) of both the samples, i.e., pure curcumin and Cr-NLC, is calculated by the Scherrer equation (Eq. 2) and is found to be 93.029% and 64%, respectively.

Storage stability studies

The formulated Cr-NLC dispersion was evaluated for storage stability for up to 90 days at 4 °C and 25 °C. No considerable changes in selected parameters were observed. The storage stability data of Cr-NLCs dispersion are described in Table 4. This suggested the formulated Cr-NLCs dispersion is stable on storage.

Anthelmintic assay

The efficiency of Cr-NLC as an anthelmintic agent against earthworms is presented in Table 5**.** Paralysis and mortality time in earthworms (*Pheretima posthuma*) treated with Cr-NLC were compared with standard therapeutic agent (albendazole). Cr-NLC shows potent anthelmintic

Table 4 Storage stability studies of Cr-NLCs dispersion at 4 °C and 25 °C

Factors	Day 1		After 30 days		After 60 days		After 90 days	
	25 °C	4 °C	25 °C	4 °C	25 °C	4 °C	25 °C	4 °C
P-size (nm)	144	144	151.7	152.7	152	158.4	158	159.7
PdI	0.301	0.301	0.504	0.275	0.270	0.423	0.410	0.461
Zeta potential (mV)	−33.2	−33.2	−32.3	−31.6	−31.4	−31.2	−30.7	−29.6
Entrapment efficiency (%)	92.48	92.48	91.93	91.24	90.84	91.20	89.96	90.89

Table 5 Anthelmintic study against earthworm

Formulation	Cr-NLC 10 mg/ml	Albendazole 10 mg/ml	Cr-NLC 20 mg/ml	Albendazole 20 mg/ml	Saline
Paralysis time (mean ± SEM)	18 min 15 s ± 32 s	14 min 55 s ± 21	16 min 31 s ± 30 s	12 min 17 s ± 30 s	Alive
Mortality time (mean ± SEM)	39 min 28 s ± 20 s	35 min 48 s ± 29	34 min 24 s ± 35 s	31 min 33 s ± 35 s	Alive

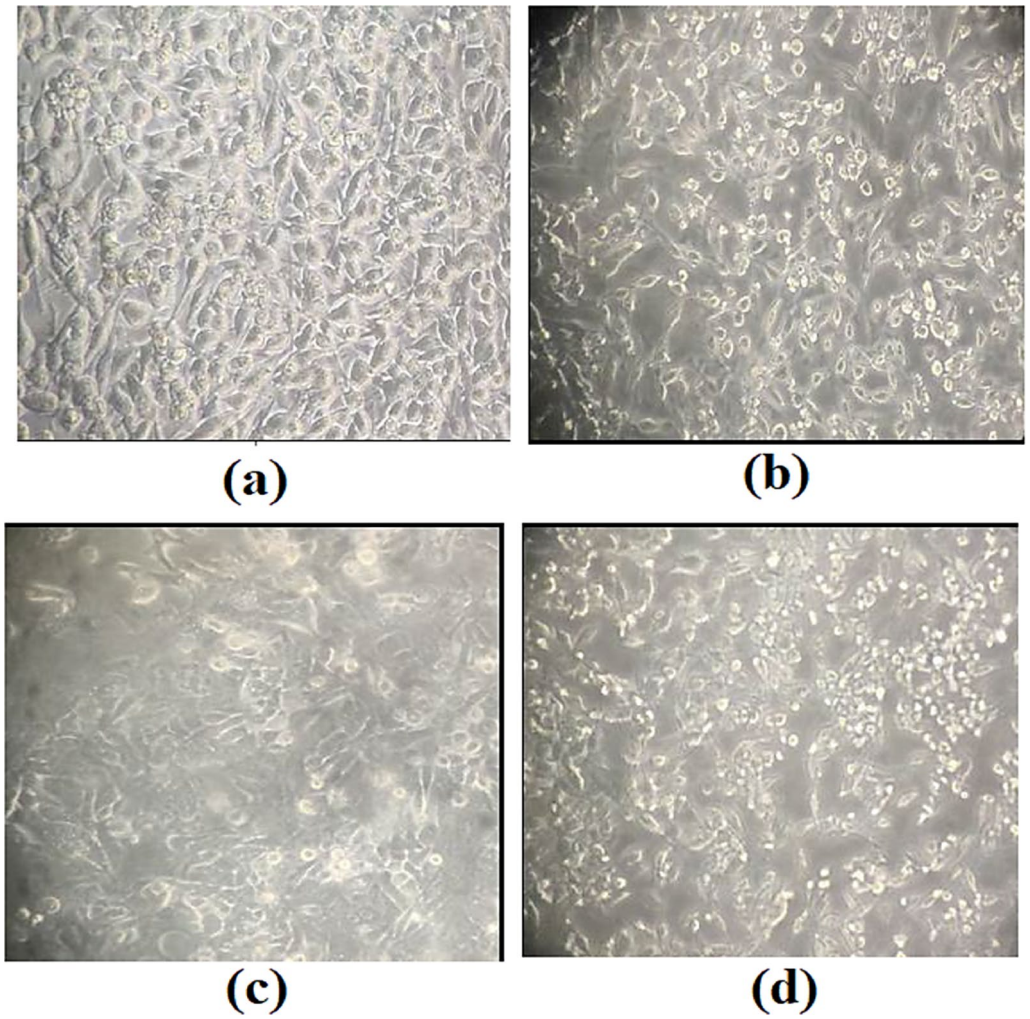

Fig. 10 **a**, **c** shows untreated control cells (Vero) and **b**, **d** in the presence of curcumin and Cr-NLC, respectively, at 80 µg/ml after 24 h

activity in a dose-dependent manner. There were very slight differences in anthelmintic potential between the tested formulation and standard drug. These data suggest that curcumin-loaded NLC may be a promising candidate for parasitic disease. Saline-treated earthworms showed normal physical activity and remained active throughout experiments.

Cytotoxicity study

The growth of Vero E6 cells treated with Cr-NLC and pure curcumin (used in the concentration range of 10–80 µg/ml) was compared to that of untreated healthy Vero cells and assessed in terms of IC_{50} value. The IC_{50} value of pure curcumin and Cr-NLC was found to be 350.99 and 285.88 µg/ml ($IC_{50} > 100$ µg/ml) which is considered to be nontoxic for both the samples [63, 64] in the concentration range taken. Morphological analysis of Vero cells of control or normal cells (Fig. 10a, c) is compared with Cr-NLC treated cells (Fig. 10b, d) at 80 µg/ml concentration displayed in Fig. 10 showing no significant change in cell morphology. Figure 11 shows a graph of the % viability of Vero cells incubated with Cr-NLC and pure curcumin at different drug concentrations. It can be inferred from Fig. 11 that curcumin and Cr-NLC do not inhibit the growth of Vero cells at any concentration (up to 80 µg/ml) and show more than 85% cell viability. So, the formulation is considered to be safe. The literature also reports that curcumin is safe for normal cells and no cytotoxicity was perceived up to a dose of 500 µg/mL [64–66].

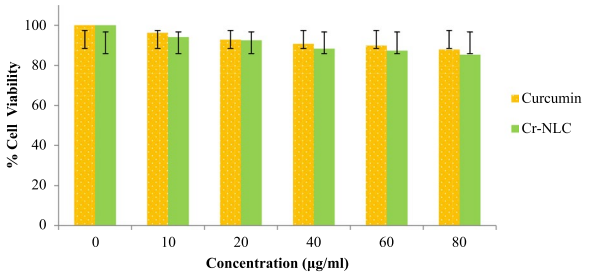

Fig. 11 Dose-dependent effect of curcumin and Cr-NLC on viability of Vero cells in vitro using MTT assay

Discussion

In this work, curcumin-loaded NLCs were fabricated using a single-step, one-pot microwave-assisted approach. Beeswax and oleic acid were used as solid and liquid lipids, respectively, while Tween 80 was used as surfactant. The formulation was optimized using 2 factors 3 levels of central composite design (CCD). The concentration of lipid blend (X_1) and concentration of surfactant (X_2) were selected as formulation variables and taken into consideration at three different levels (−1, 0, 1). The average p-size (Y_1), PdI (Y_2), and zeta potential (ζ) (Y_3) were designated as responses (Table 1). For every batch of NLC formulation, the average p-size, PdI, % EE, and zeta potential (ζ) were calculated. The average p-size range varies from 144 to 520 nm with monodispersity of the formulation, also the value of zeta potential of all the batches lies in the range of − 25.3 to − 33.2 mV. The % EE of all the batches lies in the range from 92.4 ± 0.2% to 98.3 ± 0.3%, thus indicating that a significant amount of drug has been entrapped in each batch. FT-IR analysis was performed to identify any interactions between the drug and the formulation excipients. The result revealed that there is no chemical interaction between the drug and the formulation excipients.

The XRD pattern of pure curcumin exhibited well-defined, intense sharp peaks whereas XRD spectra of Cr-NLC revealed a more disordered or amorphous state of the formulation. The HR-TEM images revealed spherical particles ranging from 10 to 200 nm in size (Fig. 5). A study was conducted on earthworms to determine the anthelmintic potential of Cr-NLC in comparison with albendazole. The results showed that Cr-NLC exhibits potent anthelmintic activity in a dose-dependent manner. Additionally, a cytotoxicity study was carried out on Vero cells, and the results were evaluated in terms of IC_{50} value. The study confirmed that the formulation is nontoxic to Vero cells, indicating its safety. An in vitro drug release study showed 90.76 ± 0.01% release of curcumin in 24 h by following the Korsmeyer-Peppas model of release kinetics. The storage stability of any formulation is an essential component. The storage stability of the formulated Cr-NLC dispersion was evaluated at 4 °C and 25 °C for up to 90 days. No considerable changes in selected parameters were observed. The above-mentioned results suggest that NLCs developed using the microwave approach could be effective drug carriers for the treatment of parasitic infections through topical and oral administration potentially serving as an alternative treatment for other parasite diseases.

Conclusion

In the present investigation, nanostructured lipidic carriers containing curcumin were fabricated using a microwave-assisted procedure employing a central composite experimental design. The Cr-NLC demonstrated nanoscale size formulation, narrow size distribution, excellent entrapment efficiency, and sufficient surface electrostatic potential to prevent accumulation with augmented physical stability. The spherical form of the particles was seen in TEM micrographs. In vitro, drug release study displayed sustained release till 24 h whereas in vivo study carried out against earthworms, possessing close anatomical and physiological similarity with human intestinal parasites, exhibited anthelmintic potential. Cytotoxicity studies also declared the formulation to be nontoxic to Vero cells. Hence, the single-step one-pot microwave-assisted technique produced curcumin-loaded NLCs with improved physical stability and modified drug release properties bear the anthelmintic potential and are nontoxic and can further be explored as a potential substitute for the treatment of other parasitic illnesses.

Future prospects

Due to prevailing parasitic infections, the treatment regime may be either topical or oral. Cr-NLCs may be explored as injectable preparations. Future studies may be focused more on improving the bioavailability of curcumin.

Abbreviations

C. longa	*Curcuma longa*
Cr-NLC	Curcumin-loaded nanostructured lipid carriers
Eq	Equation
Fig	Figure
GRAS	Generally recognized as safe
NLCs	Nanostructured lipid carriers
PdI	Polydispersity Index
P-size	Particle size
R^2 value	Regression coefficient value
Rpm	Rotation per minute
SEM	Standard error of the mean
SLNs	Solid lipid nanoparticles

Acknowledgements

Not applicable

Author contributions
SL was involved in the conceptualization, investigation, and writing—original drafts preparation. RV contributed to the reviewing and editing. DK assisted in reviewing and editing. MB contributed to the conceptualization, supervision, reviewing and editing.

Funding
This study did not receive any funding from any sector.

Declarations

Ethics approval and consent to participate
Not applicable.

Consent for publication
Not applicable.

Competing interest
No competing interest to disclose.

Author details
[1]Department of Pharmaceutical Sciences, Guru Jambheshwar University of Science & Technology, Hisar 125001, India. [2]Department of Pharmaceutical Sciences, Chaudhary Bansi Lal University, Bhiwani 127021, India. [3]Department of Pharmaceutical Sciences, Maharshi Dayanand University, Rohtak 124001, India.

Received: 29 October 2023 Accepted: 10 December 2023
Published online: 15 December 2023

References

1. Caldrer S, Ursini T, Santucci B, Motta L, Angheben A (2022) Soil-transmitted helminths and anaemia: a neglected association outside the tropics. Microorganisms 10(5):1027. https://doi.org/10.3390/microorganisms10051027
2. Buonfrate D, Gobbi F, Marchese V, Postiglione C, Badona Monteiro G, Giorli G, Napoletano G, Bisoffi Z (2018) Extended screening for infectious diseases among newly-arrived asylum seekers from Africa and Asia, Verona province, Italy, April 2014 to June 2015. Euro Surveill 23(16):17–00527. https://doi.org/10.2807/1560-7917.ES.2018.23.16.17-00527
3. Van Wyk BE, Wink M (2018) Medicinal plants of the world. An illustrated scientific guide to important medicinal plants and their uses. Timber Press, Portland
4. Taylor JLS, Rabe T, McGaw LJ, Jäger AK, Van Staden J (2001) Towards the scientific validation of traditional medicinal plants. Plant Growth Regul 34:23–37. https://doi.org/10.1023/A:1013310809275
5. Cheraghipour K, Marzban A, Ezatpour B, Khanizadeh S, Koshki J (2018) Antiparasitic properties of curcumin: a review. AIMS Agric Food 4(561.10):3934
6. Tabanelli R, Brogi S, Calderone V (2021) Improving curcumin bioavailability: current strategies and future perspectives. Pharmaceutics 13(10):1715. https://doi.org/10.3390/pharmaceutics13101715
7. Hassanzadeh K, Buccarello L, Dragotto J, Mohammadi A, Corbo M, Feligioni M (2020) Obstacles against the marketing of curcumin as a drug. Int J Mol Sci 21(18):6619. https://doi.org/10.3390/ijms21186619
8. Vijayakumar S, Malaikozhundan B, Saravanakumar K, Durán-Lara EF, Wang MH, Vaseeharan B (2019) Garlic clove extract assisted silver nanoparticle: antibacterial, antibiofilm, antihelminthic, anti-inflammatory, anticancer and ecotoxicity assessment. J Photochem Photobiol 198:111558. https://doi.org/10.1016/j.jphotobiol.2019.111558
9. Kayser O, Kiderlen AF, Croft SL (2002) Natural products as potential antiparasitic drugs. Stud Natl Prod Chem 26:779–848. https://doi.org/10.1016/S1572-5995(02)80019-9
10. Rai M, Ingle AP, Pandit R, Paralikar P, Anasane N, Santos CAD (2020) Curcumin and curcumin-loaded nanoparticles: antipathogenic and antiparasitic activities. Expert Rev Anti Infect Ther 18(4):367–379. https://doi.org/10.1080/14787210.2020.1730815
11. Anand P, Kunnumakkara AB, Newman RA, Aggarwal BB (2007) Bioavailability of curcumin: problems and promises. Mol Pharm 4(6):807–818. https://doi.org/10.1021/mp700113r
12. Strimpakos AS, Sharma RA (2008) Curcumin: preventive and therapeutic properties in laboratory studies and clinical trials. Antioxid Redox Signal 10(3):511–545. https://doi.org/10.1089/ars.2007.1769
13. Chen C, Johnston TD, Jeon H, Gedaly R, McHugh PP, Burke TG, Ranjan D (2009) An in vitro study of liposomal curcumin: stability, toxicity and biological activity in human lymphocytes and Epstein-Barr virus-transformed human B-cells. Int J Pharm 366(1–2):133–139. https://doi.org/10.1016/j.ijpharm.2008.09.009
14. Rudramurthy GR, Swamy MK (2018) Potential applications of engineered nanoparticles in medicine and biology: an update. J Biol Inorg Chem 23(8):1185–1204. https://doi.org/10.1007/s00775-018-1600-6
15. Zajdel K, Janowska J, Frontczak-Baniewicz M, Sypecka J, Sikora B (2023) Upconverting nanoparticles as a new bio-imaging strategy-investigating intracellular trafficking of endogenous processes in neural tissue. Int J Molecular Sci 24(2):1122. https://doi.org/10.3390/ijms24021122
16. Patra JK, Das G, Fraceto LF, Campos EVR, Rodriguez-Torres MDP, Acosta-Torres LS, Diaz-Torres LA, Grillo R, Swamy MK, Sharma S, Habtemariam S, Shin HS (2018) Nano based drug delivery systems: recent developments and future prospects. J Nanobiotechnology 16(1):71. https://doi.org/10.1186/s12951-018-0392-8
17. Jahangirian H, Lemraski EG, Webster TJ, Rafiee-Moghaddam R, Abdollahi Y (2017) A review of drug delivery systems based on nanotechnology and green chemistry: green nanomedicine. Int J Nanomedicine 12:2957–2978. https://doi.org/10.2147/IJN.S127683
18. Shirodkar RK, Kumar L, Mutalik S, Lewis S (2019) Solid lipid nanoparticles and nanostructured lipid carriers: emerging lipid based drug delivery systems. Pharm Chem J 53(5):440
19. Yoon G, Park JW, Yoon IS (2013) Solid lipid nanoparticles (SLNs) and nanostructured lipid carriers (NLCs): recent advances in drug delivery. J Pharm Investig 43:353–362
20. Yang Y, Corona A 3rd, Schubert B, Reeder R, Henson MA (2014) The effect of oil type on the aggregation stability of nanostructured lipid carriers. J Colloid Interface Sci 418:261–272. https://doi.org/10.1016/j.jcis.2013.12.024
21. Bhatia M, Kumar S, Kapoor A, Lohan S (2022) A review on the drug delivery strategies for parasitic infections: scope and assertion. Drug Deliv Lett 12(2):109–121. https://doi.org/10.2174/2210303112666220329154123
22. Haider M, Abdin SM, Kamal L, Orive G (2020) Nanostructured lipid carriers for delivery of chemotherapeutics: a review. Pharmaceutics 12(3):288. https://doi.org/10.3390/pharmaceutics12030288
23. Shrestha H, Bala R, Arora S (2014) Lipid-based drug delivery systems. J Pharm 2014:801820. https://doi.org/10.1155/2014/801820
24. Patidar A, Thakur DS, Kumar P, Verma J (2010) A review on novel lipid based nanocarriers. Int J Pharm Pharm Sci 2(4):30–35
25. Soleimanian Y, Goli SAH, Varshosaz J, Sahafi SM (2018) Formulation and characterization of novel nanostructured lipid carriers made from beeswax, propolis wax and pomegranate seed oil. Food Chem 244:83–92. https://doi.org/10.1016/j.foodchem.2017.10.010
26. Varela-Fernández R, García-Otero X, Díaz-Tomé V, Regueiro U, López-López M, González-Barcia M, Isabel Lema M, Javier Otero-Espinar F (2022) Lactoferrin-loaded nanostructured lipid carriers (NLCs) as a new formulation for optimized ocular drug delivery. Eur J Pharm Biopharm 172:144–156. https://doi.org/10.1016/j.ejpb.2022.02.010
27. Rao RR, Pisay M, Kumar S, Kulkarni S, Pandey A, Kulkarni VI, Mutalik S (2022) Medium and large scale preparation of nanostructured lipid carriers of asenapine maleate: quality-by-design based optimization, production, characterization and performance evaluation. J Drug Deliv Sci Tech 71:103275. https://doi.org/10.1016/j.jddst.2022.103275
28. Truong CT, Nguyen DTD, Vo MT, Huynh BT, Thi TAN, Do MHV, Nguyen DH (2022) Development of topical gel containing Capsicum oleoresin encapsulated Tamanu nanocarrier and its analgesic and anti-inflammatory activities. Mater Today Commun 31:103404. https://doi.org/10.1016/j.mtcomm.2022.103404
29. Jitta SR, Bhaskaran NA, Salwa, Kumar L (2022) Anti-oxidant containing nanostructured lipid carriers of ritonavir: development, optimization, and in vitro and in vivo evaluations. AAPS PharmSciTech 23(4):88. https://doi.org/10.1208/s12249-022-02240-w
30. Syed Azhar SNA, Ashari SE, Zainuddin N, Hassan M (2022) Nanostructured lipid carriers-hydrogels system for drug delivery: nanohybrid technology perspective. Molecules (Basel, Switzerland) 27(1):289. https://doi.org/10.3390/molecules27010289

31. Shah RM, Eldridge DS, Palombo EA, Harding IH (2017) Microwave-assisted microemulsion technique for production of miconazole nitrate- and econazole nitrate-loaded solid lipid nanoparticles. Eur J Pharm Biopharm 117:141–150. https://doi.org/10.1016/j.ejpb.2017.04.007
32. Islam MS, Mitra S (2023) Synthesis of microwave functionalized, nanostructured polylactic co-glycolic acid (*nf*PLGA) for incorporation into hydrophobic dexamethasone to enhance dissolution. Nanomaterials (Basel, Switzerland) 13(5):943. https://doi.org/10.3390/nano13050943
33. Khan S, Baboota S, Ali J, Khan S, Narang RS, Narang JK (2015) Nanostructured lipid carriers: an emerging platform for improving oral bioavailability of lipophilic drugs. Int J Pharm Investig 5(4):182–191. https://doi.org/10.4103/2230-973X.167661
34. Patel D, Dasgupta S, Dey S, Ramani YR, Ray S, Mazumder B (2012) Nanostructured lipid carriers (NLC)-based gel for the topical delivery of aceclofenac: preparation, characterization, and in vivo evaluation. Sci Pharm 80(3):749–764. https://doi.org/10.3797/scipharm.1202-12
35. Shah KA, Date AA, Joshi MD, Patravale VB (2007) Solid lipid nanoparticles (SLN) of tretinoin: potential in topical delivery. Int J Pharm 345(1–2):163–171. https://doi.org/10.1016/j.ijpharm.2007.05.061
36. Dantas IL, Bastos KTS, Machado M, Galvao JG, Lima AD, Gonsalves JKMC, Lira AAM (2018) Influence of stearic acid and beeswax as solid lipid matrix of lipid nanoparticles containing tacrolimus. J Therm Anal Calorim 132:1557–1566. https://doi.org/10.1007/s10973-018-7072-7
37. Dobreva M, Stefanov S, Andonova V (2020) Natural lipids as structural components of solid lipid nanoparticles and nanostructured lipid carriers for topical delivery. Curr Pharm Des 26(36):4524–4535. https://doi.org/10.2174/1381612826666200514221649
38. Chauhan I, Singh L (2023) A comprehensive literature review of lipids used in the formulation of lipid nanoparticles. Curr Nanomater 8(2):126–152. https://doi.org/10.2174/2405461507666220606164446
39. Ma P, Zeng Q, Tai K, He X, Yao Y, Hong X, Yuan F (2018) Development of stable curcumin nanoemulsions: effects of emulsifier type and surfactant-to-oil ratios. J Food Sci Techno 55(9):3485–3497. https://doi.org/10.1007/s13197-018-3273-0
40. Thomas L, Zakir F, Mirza MA, Anwer MK, Ahmad FJ, Iqbal Z (2017) Development of curcumin loaded chitosan polymer based nanoemulsion gel: in vitro, ex vivo evaluation and in vivo wound healing studies. Int J Biol Macromol 101:569–579. https://doi.org/10.1016/j.ijbiomac.2017.03.066
41. Sharma M, Mundlia J, Kumar T, Ahuja M (2021) A novel microwave-assisted synthesis, characterization and evaluation of luliconazole-loaded solid lipid nanoparticles. Polym Bull 78:2553–2567. https://doi.org/10.1007/s00289-020-03220-5
42. Shah RM, Eldridge DS, Palombo EA, Harding IH (2022) Stability mechanisms for microwave-produced solid lipid nanoparticles. Colloids Surf A 643:128774. https://doi.org/10.1016/j.colsurfa.2022.128774
43. Aldawsari HM, Singh S (2020) Rapid microwave-assisted cisplatin-loaded solid lipid nanoparticles: synthesis, characterization and anticancer study. Nanomaterials (Basel, Switzerland) 10(3):510. https://doi.org/10.3390/nano10030510
44. Kesharwani D, Paul SD, Paliwal R, Satapathy T (2023) Development, QbD based optimization and *in vitro* characterization of Diacerein loaded nanostructured lipid carriers for topical applications. J Radiat Res Applied Sci 16(2):100565. https://doi.org/10.1016/j.jrras.2023.100565
45. Upadhyay C, D'Souza A, Patel P, Verma V, Upadhayay KK, Bharkatiya M (2023) Inclusion complex of ibuprofen-β-cyclodextrin incorporated in gel for mucosal delivery: optimization using an experimental design. AAPS PharmSciTech 24(4):100. https://doi.org/10.1208/s12249-023-02534-7
46. Verma R, Mittal V, Kaushik D (2017) Self-micro emulsifying drug delivery system: a vital approach for bioavailability enhancement. Int J ChemTech Res 10(7):515–528
47. Verma R, Kaushik D (2019) Development, optimization, characterization and impact of in vitro lipolysis on drug release of telmisartan loaded SMEDDS. Drug Deliv Lett 9(4):330–340
48. Madane RG, Mahajan HS (2016) Curcumin-loaded nanostructured lipid carriers (NLCs) for nasal administration: design, characterization, and in vivo study. Drug Deliv 23(4):1326–1334. https://doi.org/10.3109/10717544.2014.975382
49. Nadaf SJ, Killedar SG (2018) Curcumin nanocochleates: use of design of experiments, solid state characterization, *in vitro* apoptosis and cytotoxicity against breast cancer MCF-7 cells. J Drug Deliv Sci Technol 47:337–350. https://doi.org/10.1016/j.jddst.2018.06.026
50. Lee HJ, Jeong M, Na YG, Kim SJ, Lee HK, Cho CW (2020) An EGF- and curcumin-co-encapsulated nanostructured lipid carrier accelerates chronic-wound healing in diabetic rats. Molecules (Basel, Switzerland) 25(20):4610. https://doi.org/10.3390/molecules25204610
51. Verma R, Kaushik A, Almeer R, Rahman MH, Abdel-Daim MM, Kaushik D (2021) Improved pharmacodynamic potential of rosuvastatin by self-nanoemulsifying drug delivery system: an in vitro and in vivo evaluation. Int J Nanomed 16:905–924
52. Gupta T, Singh J, Kaur S, Sandhu S, Singh G, Kaur IP (2020) Enhancing bioavailability and stability of curcumin using solid lipid nanoparticles (clen): a covenant for its effectiveness. Front Bioeng Biotechnol 8:879. https://doi.org/10.3389/fbioe.2020.00879
53. Verma R, Kaushik D (2021) Design and optimization of candesartan loaded self-nanoemulsifying drug delivery system for improving its dissolution rate and pharmacodynamic potential. Drug Deliv 27(1):756–771. https://doi.org/10.1080/10717544.2020.1760961
54. Bazh EK, El-Bahy NM (2013) *In vitro* and *in vivo* screening of anthelmintic activity of ginger and curcumin on *Ascaridia galli*. Parasitol Res 112(11):3679–3686. https://doi.org/10.1007/s00436-013-3541-x
55. Vadakkan K, Cheruvathur MK, Chulliparambil AS, Francis F, Abimannue AP (2021) Proteolytic enzyme arbitrated antagonization of helminthiasis by *Cinnamomum cappara* leaf extract in *Pheretima posthuma*. Clin Phytoscience 7(1):1–9. https://doi.org/10.1186/s40816-021-00261-9
56. Ajaiyeoba EO, Onocha PA, Olarenwaju OT (2001) In vitro anthelmintic properties of *Buchholzia coriaceae* and *Gynandropsis gynandra* extracts. Pharm Biol 39(3):217–220. https://doi.org/10.1076/phbi.39.3.217.5936
57. Kode J, Kovvuri J, Nagaraju B, Jadhav S, Barkume M, Sen S, Kamal A (2020) Synthesis, biological evaluation, and molecular docking analysis of phenstatin based indole linked chalcones as anticancer agents and tubulin polymerization inhibitors. Bioorg Chem 105:104447. https://doi.org/10.1016/j.bioorg.2020.104447
58. Aditya NP, Shim M, Lee I, Lee Y, Im MH, Ko S (2013) Curcumin and genistein coloaded nanostructured lipid carriers: in vitro digestion and antiprostate cancer activity. J Agricult Food Chem 61(8):1878–1883. https://doi.org/10.1021/jf305143k
59. Rahman MA, Ali A, Rahamathulla M, Salam S, Hani U, Wahab S, Harwansh RK (2023) Fabrication of sustained release curcumin-loaded solid lipid nanoparticles (cur-SLNs) as a potential drug delivery system for the treatment of lung cancer: optimization of formulation and in vitro biological evaluation. Polymers 15(3):542. https://doi.org/10.3390/polym15030542
60. Maia M, Barros AI, Nunes FM (2013) A novel, direct, reagent-free method for the detection of beeswax adulteration by single-reflection attenuated total reflectance mid-infrared spectroscopy. Talanta 107:74–80. https://doi.org/10.1016/j.talanta.2012.09.052
61. Behbahani ES, Ghaedi M, Abbaspour M, Rostamizadeh K, Dashtian K (2019) Curcumin loaded nanostructured lipid carriers: In vitro digestion and release studies. Polyhedron 164:113–122. https://doi.org/10.1016/j.poly.2019.02.002
62. Wijiani N, Isadiartuti D, Rijal MAS, Yusuf H (2020) Characterization and dissolution study of micellar curcumin-spray dried powder for oral delivery. Int J Nanomed 15:1787–1796. https://doi.org/10.2147/IJN.S245050
63. Grover M, Behl T, Sehgal A, Singh S, Sharma N, Virmani T, Bungau S (2021) In vitro phytochemical screening, cytotoxicity studies of *Curcuma longa* extracts with isolation and characterisation of their isolated compounds. Molecules 26(24):7509. https://doi.org/10.3390/molecules26247509
64. Ahmad R, Srivastava AN, Khan MA (2016) Evaluation of in vitro anticancer activity of rhizome of *Curcuma longa* against human breast cancer and Vero cell lines. Evaluation 1(1):01–06
65. Mahmoud S, Hassab El-Nabi S, Hawash A, El-Seedi HR, Khalifa SA, Ullah S, El-Garawani IM (2022) Curcumin-injected *Musca domestica* larval hemolymph: Cecropin upregulation and potential anticancer effect. Molecules 27(5):1570. https://doi.org/10.3390/molecules27051570
66. Jain R (2013) Nature identical curcumin. Int J Appl Basic Med Res 3(2):134. https://doi.org/10.4103/2229-516X.117104

Publisher's Note